Histological and immunohistochemical features suggesting aetiological differences in lymph node and (muco)cutaneous feline tuberculosis lesions

PETSAVERS PAPER

Histological and immunohistochemical features suggesting aetiological differences in lymph node and (muco) cutaneous feline tuberculosis lesions

J. L. Mitchell [1,*], J. Del Pozo*, C. S. C. Woolley*, R. Dheendsa*, J. C. Hope* and D. A. Gunn-Moore*

*Royal (Dick) School of Veterinary Studies and The Roslin Institute, The University of Edinburgh, Easter Bush, Midlothian EH25 9RG, UK

[1]Corresponding author email: jordan.mitchell@ed.ac.uk

Objectives: To identify and describe histological and immunohistochemical criteria that may differentiate between skin and lymph node lesions associated with *Mycobacterium* (*M.*) *bovis* and *M. microti* in a diagnostic pathology setting.

Materials and Methods: Archived skin and lymph node biopsies of tuberculous lesions were stained with haematoxylin and eosin, Ziehl-Neelsen and Masson's Trichrome. Immunohistochemistry was performed to detect the expression of calprotectin, CD3 and Pax5. Samples were scored for histological parameters (*i.e.* granulomas with central necrosis versus small granulomas without central necrosis, percentage necrosis and/or multinucleated giant cells), number of acid-fast bacilli (bacterial index) and lesion percentage of fibrosis and positive immunohistochemical staining.

Results: Twenty-two samples were examined (*M. bovis* n=11, *M. microti* n=11). When controlling for age, gender and tissue, feline *M. bovis*-associated lesions more often featured large multi-layered granulomas with central necrosis. Conversely, this presentation was infrequent in feline *M. microti*-associated lesions, where small granulomas without central necrosis predominated. The presence of an outer fibrous capsule was variable in both groups, as was the bacterial index. There were no differences in intralesional expression of immunohistochemical markers.

Clinical Significance: Differences in the histological appearance of skin and lymph node lesions may help to infer feline infection with either *M. bovis* or *M. microti* at an earlier stage when investigating these cases, informing clinicians of the potential zoonotic risk. Importantly, cases of tuberculosis can present with numerous acid-fast bacilli. This implies that a high bacterial index does not infer infection with non-zoonotic non-tuberculous mycobacteria.

Journal of Small Animal Practice (2021), 1–14
DOI: 10.1111/jsap.13386

Accepted: 16 May 2021

INTRODUCTION

Mycobacterial infections are increasingly recognised as a substantial cause of morbidity in the domestic cat population, especially in Great Britain (Broughan *et al.* 2013), where approximately 1% of all feline biopsy submissions show changes suggestive of mycobacterial disease (Gunn-Moore *et al.* 2013). The most common presentation of feline mycobacteriosis is raised cutaneous lesions; these may be ulcerated and discharging sinus tracts can be present. Local lymphadenitis is frequently identified, presumptively due to drainage of mycobacteria-laden immune cells, which are predominantly macrophages (Ganbat *et al.* 2016), from the cuta-

JSAP JOURNAL OF SMALL ANIMAL PRACTICE

neous lesion (Gunn-Moore *et al*. 2011a). This clinical presentation is recognised in cases of infection with members of the *Mycobacterium* (*M*.) *tuberculosis*-complex (MTBC) as well as non-tuberculous mycobacteria (NTM) such as members of the *M. avium*-complex (Gunn-Moore 2014). Infection can spread to the lungs, putatively due to haematogenous spread within monocytes and neutrophils (Latimer *et al*. 1997, Krishnan *et al*. 2010), resulting in a broncho-interstitial pulmonary pattern (Bennett *et al*. 2011). Mycobacterial lesions have also been reported in the eyes (Stavinohova *et al*. 2019), joints (Lalor *et al*. 2017) and other organs and tissues, resulting in a range of clinical signs (Gunn-Moore 2014).

The MTBC consists of 10 different mycobacterial species (Rodriguez-Campos *et al*. 2014, Dippenaar *et al*. 2015), responsible for causing tuberculosis (TB) across a wide taxon of animals. Those that cause TB in the domestic cat are *M. bovis* and *M. microti*, the vole bacillus (Gunn-Moore *et al*. 2011a), both of which are potentially zoonotic (Emmanuel *et al*. 2007, O'Connor *et al*. 2019). While *M. bovis* has been identified as causing disease across multiple species of veterinary interest, reports of *M. microti* infection in species other than the domestic cat and its maintenance host the field vole (*Microtus agrestis*) are uncommon, although they are being identified more frequently (Smith *et al*. 2009, Boniotti *et al*. 2014, Michelet *et al*. 2015). Where positive culture results were obtained, over 70% of feline mycobacterial infections in Great Britain were due to MTBC pathogens, fairly evenly distributed between *M. microti* and *M. bovis* (approximately 40% and 33%, respectively) (Gunn-Moore *et al*. 2011a). These appear to localise to specific regions of the UK; *M. bovis* is more frequent in cats from TB endemic areas, whereas *M. microti* infection is more frequent in cats from areas with low or null prevalence of bovine TB (*i.e*. Scotland), (Burthe *et al*. 2008).

M. bovis and *M. microti* infections produce identical macroscopic lesions; however, they differ in their zoonotic potential, and for some owners the decision to treat or euthanise their cat can depend on whether *M. bovis* is demonstrated as the infective organism (O'Halloran & Gunn-Moore 2017). Therefore, the ability to rapidly discern between the two causative agents of feline TB is essential and can inform the potential risk posed to owners as well as veterinary staff (de la Rua-Domenech 2006).

Histopathology is often the first diagnostic test performed when investigating a potential case of mycobacterial disease in cats (Gunn-Moore 2014, O'Halloran & Gunn-Moore 2017), and lesions featuring granulomatous to pyogranulomatous inflammation, dominated by epithelioid macrophages, raise the suspicion index of mycobacterial disease (Gunn-Moore *et al*. 2011b). Unlike in other species, multinucleated giant cells (MNGCs) are not routinely observed in feline mycobacterial lesions (Kipar *et al*. 2003). Special stains, such as Ziehl-Neelsen (ZN), can be performed on sections where granulomatous to pyogranulomatous inflammation is identified to confirm the presence of acid-fast bacilli (AFB) morphologically consistent with mycobacteria. However, many feline mycobacterial lesions are paucibacillary, *i.e*. they have few to no obvious AFB on ZN-staining, so a negative result does not rule out mycobacteriosis (Gunn-Moore *et al*. 2013). Abundant numbers of AFB, where identified, have been associated with cases of lepromatous feline leprosy, a disease entity caused by non-zoonotic NTM species (Malik *et al*. 2002, O'Brien *et al*. 2017).

Subsequent diagnostic testing for feline mycobacterial infections can be challenging. Specialist culture, which is the validated assay, has poor sensitivity (Gunn-Moore *et al*. 2011a) and it can take at least 3 months to obtain a positive result for slow-growing mycobacterial species, which includes *M. microti* (Smith *et al*. 2009). More rapid testing methodologies are available, including molecular-based diagnostics, such as polymerase chain reaction (PCR) assays (Aranaz *et al*. 1996, Richter *et al*. 2003); however, they are less sensitive on formalin-fixed tissues compared to fresh samples (Reppas *et al*. 2013). Recent advancements in molecular biology have improved the ability of tests to discriminate between members of the MTBC, resulting in an increase in the identification of *M. microti* as a causative agent of TB lesions across a range of species (Boniotti *et al*. 2014, Michelet *et al*. 2015, Landolt *et al*. 2019, Pérez De Val *et al*. 2019). Despite this, the financial constraints of owners may limit the use of these techniques for the species-level diagnosis of feline mycobacterial infections. The interferon-gamma (IFNγ) release assay (IGRA) has excellent sensitivity for detecting MTBC infections and is reasonable at differentiating between *M. bovis* and *M. microti*; however, financial constraints may still apply, obtaining sufficient volumes of blood may be a limiting factor in some cats, and the test requires careful handling and processing of heparinised blood (Rhodes *et al*. 2008, Rhodes *et al*. 2011).

The hallmark of TB is granulomatous inflammation; this term can encompass a range of histopathological presentations, from unorganised macrophage infiltration, to the presence of well-formed granulomas (Shah *et al*. 2017). A precise definition for what constitutes a granuloma is difficult, but at its simplest, the granuloma can be thought of as "an organised collection of mature mononuclear phagocytic cells" (Adams 1976, Pagán & Ramakrishnan 2018). Tuberculous granulomas typically consist of epithelioid macrophages surrounding a necrotic core, encapsulated by fibroblasts and an outer layer of lymphocytes (Martin *et al*. 2016). The tuberculous granuloma within lymph nodes has been well described in cattle (Wangoo *et al*. 2005) and these histological findings have been applied to a number of other livestock (Sanchez *et al*. 2011, Vallejo *et al*. 2018) and wildlife species (Canfield *et al*. 2002, García-Jiménez *et al*. 2012, García-Jiménez *et al*. 2013).

The granuloma can be characterised further by its cellular composition using immunohistochemistry (IHC). This has been performed extensively in both experimental and natural *M. bovis* infections of livestock (Pereira-Suárez *et al*. 2006, Palmer *et al*. 2007, Sanchez *et al*. 2011, Canal *et al*. 2017, Vallejo *et al*. 2018) and wildlife species (Canfield *et al*. 2002, García-Jiménez *et al*. 2012, García-Jiménez *et al*. 2013), as well as one study describing *M. microti* lesions in its natural host, the field vole (Kipar *et al*. 2014). One study has been performed on feline mycobacterial lesions (Kipar *et al*. 2003); however, this did not explore differences between *M. bovis* and *M. microti* infections.

The objective of the current study was to describe and compare the histological and immunohistochemical features of feline tuberculous granulomas in (muco)cutaneous and lymph node lesions to identify potential patterns that help differentiate between the two causes of TB in cats. We hypothesise that the nodal/(muco)cutaneous granulomas observed in cats infected with *M. microti* differ in structural organisation and immune cell populations compared to those in *M. bovis*-positive cats.

MATERIALS AND METHODS

Animals and samples

Ethical approval for this study was granted by the institutional Veterinary Ethical Review Committee (approval no. 79 14).

A database maintained on Microsoft Excel © 2016 (Microsoft Corporation) by an independent researcher was searched by the lead investigator in May 2019 to identify cats where a formalin-fixed paraffin-embedded (FFPE) tuberculous (muco)cutaneous or lymph node lesion biopsy had been submitted to the institution by referring veterinary surgeons (RVS) and commercial histopathology laboratories following owner consent, and that had a culture, PCR or IGRA diagnosis of *M. bovis* or *M. microti* infection. (Muco)cutaneous biopsies were taken to include those recorded as being "skin," "dermal," "subcutaneous" and "gum". The biopsies had been taken as part of the diagnostic investigation of these cases or at *post-mortem* examination and were fixed in 10% neutral buffered formalin for a minimum of 24 hours post-sampling and processed for histology using standard methods. Anti-mycobacterial therapy had not been given before sampling. Mycobacterial disease was suspected based on histopathological examination and/or ZN-staining, and subsequent speciation was confirmed by external specialist mycobacterial culture (Animal and Plant Health Agency), PCR (Leeds Teaching Hospitals NHS Trust) or IGRA (Biobest Laboratories). An IGRA diagnosis of *M. microti* was considered definitive if the IGRA result showed a biased response to purified protein derivative (PPD) from *M. bovis* (PPDB) over PPD from *M. avium* (PPDA) and no response to the antigenic cocktail of early secretory antigenic target 6 kDa (ESAT-6)/culture filtrate protein 10 kDa (CFP-10) (Rhodes *et al.* 2011), the cats had lesions exhibiting histological features consistent with mycobacterial infection, and they lived in regions of England that are low-risk areas for bovine TB or in Officially TB Free regions, *i.e.* Scotland. Conversely, an IGRA diagnosis of *M. bovis* was considered definitive if the IGRA result was PPDB-biased over PPDA and ESAT-6/CFP-10 was either positive or negative (Rhodes *et al.* 2011), with histological features consistent with mycobacteriosis, and the cat had been living in an area with bovine TB. The exception to having been living in a "high-risk" or "edge" area for bovine TB, is any cat fed the raw commercial diet that has recently been associated with an outbreak of *M. bovis* in cats in England and Scotland (O'Halloran *et al.* 2019). Eligible cases were cross-referenced with clinical histories supplied by the RVS to identify additional clinical information, *i.e.* results of testing for feline leukaemia virus (FeLV) p27 antigen and feline immunodeficiency virus (FIV) anti-p24 antibodies (SNAP FIV/FeLV Combo Test, Idexx). For each cat, a single FFPE tissue block was selected; serial sections were prepared for histopathology and IHC.

Control FFPE tissues for IHC were a submandibular lymph node from a cat euthanased for reasons not related to mycobacterial infection, and a cutaneous lesion from a cat diagnosed with a NTM infection on IGRA with abundant AFB.

Histopathology

Histopathology was performed to assess the morphological features of the mycobacterial lesions (henceforth, the word lesion will always refer to a granulomatous or pyogranulomatous inflammatory infiltrate). Four-micron thick sections were cut and stained with haematoxylin and eosin (H&E), Ziehl-Neelsen (ZN) and Masson's Trichrome (MT). H&E-stained slides were evaluated to describe the cellular composition and granuloma type of the lesions, with a focus on specific parameters.

A lesion was defined as an area of infiltration by macrophages which were mostly epithelioid. The histological presentation of lesions was assessed and compared to previously described classification systems in other species (Wangoo *et al.* 2005). However, these systems did not adapt to feline tuberculous lesions, as MNGCs and dystrophic mineralisation were not present in any case. For this reason, a novel, description-based classification was devised for this study (see results). Necrosis was defined as areas with loss of cellular and structural detail, with accumulation of eosinophilic and basophilic (karyorrhectic) debris. This presentation is consistent with caseous necrosis (Miller & Zachary 2017).

Slides stained with ZN were examined under standard light microscopy to determine the bacterial index (BI). To do this, the number of individual AFB were counted in 15 randomly chosen high-power fields (hpf) (×1000 magnification) and an average was calculated (AFB/hpf). A modified Ridley BI score, used for leprosy in humans (Ridley 1964), was used to grade the number of AFB/hpf on a scale of 0 to 6: 0=no AFB/hpf; 1=0.01 to 0.1; 2=0.11 to 1.0; 3=1.01 to 10; 4=10.01 to 100; 5=100.01 to 1000; 6=>1000 AFB/hpf). In accordance with the Ridley BI score, those graded 0 to 2 were categorised as low BI and those 3 to 6 as high BI.

Slides stained with MT, to identify collagen, were analysed as described below to obtain the lesion percentage value of fibrosis.

Immunohistochemistry

IHC was performed to detect the expression of calprotectin, CD3 and Pax5. Briefly, sections were mounted on SuperFrost® Plus-coated slides (Thermo Electron Ltd.), dewaxed, rehydrated, rinsed in distilled water and then washed in Tris-buffered saline (TBS) with Tween®20 (TBS-T) (28,360, Thermo Scientific) before antigen-retrieval. All antibodies were diluted in TBS-T and all washes between steps were in TBS-T. For calprotectin, which is expressed by granulocytes, monocytes and recently blood-derived macrophages (Rugtveit *et al.* 1996), mouse monoclonal anti-human macrophages antibody, clone MAC387 (MCA874G, Bio-Rad) (Kipar *et al.* 2003) was diluted to a final concentration of 1/800 (1.25 µg/mL) and incubated for 30 minutes at room temperature (RT) follow-

ing epitope retrieval using proteinase K (S302080, Dako) for 20 minutes at RT. For CD3, a pan-T-lymphocyte marker, rabbit polyclonal anti-human CD3 antibody (A045201, Dako) (Kipar *et al*. 2003) was diluted 1/100 and incubated for 30 minutes at RT following epitope retrieval using 0.01 M sodium citrate buffer, pH 6.0 at 121°C for 40 minutes. Heat-induced epitope-retrieval (HIER) was performed using a SES Little Sister 3 autoclave (Eschmann). For Pax5 (a.k.a B-cell-specific activator protein [BSAP]) which is expressed by all stages of B-lymphocytes, although not plasma cells (Barberis *et al*. 1990), mouse monoclonal anti-human BSAP antibody, clone DAK-Pax5 (M730701) (Agostinelli *et al*. 2010) was diluted 1/50 (3.14 µg/mL) and incubated for 30 minutes at RT following HIER as for CD3. After incubation with the primary antibody, non-specific endogenous peroxidase activity was blocked using REAL Peroxidase-Blocking Solution (S202386, Dako) for 10 minutes at RT. Sections were then incubated with goat anti-mouse/anti-rabbit secondary detection polymer (EnVision™ + Dual Link System-HRP, K406311, Dako) for 45 minutes at RT, followed by visualisation of positive staining with 3,3′-diaminobenzidine tetrahydrochloride (DAB) for 10 minutes at RT. Slides were counterstained with haematoxylin and Scott's Tap Water for 10 seconds each, then dehydrated, cleared in xylene, mounted and a cover-slip was added.

Positive controls were feline tissues known to express the antigen of interest (calprotectin: an NTM-infected cutaneous lesion; CD3 and Pax5: a normal lymph node). An isotype control was used to assess non-specific staining for monoclonal antibodies, using an isotype and concentration-matched mouse anti-chicken Bu-1a/b, clone AV20 (MCA5764, Bio-Rad). Negative controls were run with omission of the primary antibody.

Image analysis

All H&E, MT and immunolabelled-slides were scanned with a NanoZoomer-XR scanner, using the NDP.scan Ver.3.2.12 software (Hamamatsu Photonics) and images viewed on NDP.view2 Ver.2.7.52 (Hamamatsu Photonics) to assess the cellular populations and granuloma type of the (pyo)granulomatous infiltrate. Quantification of necrosis and the total lesion area was determined using QuPath Ver.0.1.2 (Bankhead *et al*. 2017), with each region of interest (ROI) outlined manually using the drawing tools and the ROI file saved. To quantify the amount of fibrosis (in MT-stained sections), and the area of positive immunostaining (in IHC-stained sections), an adaptation of previously reported methods was used, using image deconvolution (Chen *et al*. 2017). Briefly, the ROI for each tissue was delineated in QuPath and sent to ImageJ (Schneider *et al*. 2012). The outside of the image was cleared, the resultant file saved and then opened in FIJI (Schindelin *et al*. 2012). For MT-stained slides, the inbuilt parameters for "Alcian Blue & H" in the colour deconvolution plug-in gave the best separation of the image file into different colour channels. The threshold for positive fibrosis staining was set as the average auto-threshold (default) for each image file; an ImageJ macro was written to quantify the area of positive staining and the total lesion area. For immunolabelled sections the "H DAB" values of the above plug-in were used and the threshold for positive staining set as the auto-threshold value for the positive control slide. ImageJ macros were then written to calculate the positive staining and total lesion areas. Isotype and negative control slides were analysed using this threshold to calculate corrections in the TB slides for any non-specific staining. All image files were visually assessed to determine accuracy of the automated analysis. Macros written for image analysis are available as Supplemental Data 1.

Statistical analysis

Data were analysed using RStudio (RStudio Team 2018). Univariate binomial logistic regression was performed to identify variables that may predict infection with either *M. bovis* or *M. microti*. Variables explored were age, gender, tissue, BI category, presence/absence of small granuloma clusters, necrosis, fibrosis, and expression of calprotectin, CD3 and Pax5. The proportion of necrosis, fibrosis and positive immunolabelling was converted to an ordinal scale variable. As age, gender and tissue were possible confounders, they were included as covariates for univariate analysis of BI category, granuloma type, necrosis, fibrosis, calprotectin, CD3 and Pax5. Multivariate logistic regression was subsequently performed on variables found to be significant on univariate analysis at $P < 0.20$, as well as the potential confounders age, gender and tissue. Variables were explored for collinearity and removed from the multivariate model where appropriate. Statistical significance for multivariate regression was set at $P < 0.05$.

RESULTS

Study population characteristics

Seventeen cats with *M. bovis* infection and 16 with *M. microti* infection with FFPE tissues available were identified from the database and assessed for eligibility. Six *M. bovis*-positive cats and two with *M. microti* were excluded as there was insufficient tissue in the FFPE block for further evaluation. Three cats diagnosed with *M. microti* on IGRA were identified as coming from high-risk areas for bovine TB and were subsequently excluded. Therefore, a total of 22 (*M. bovis* n=11, *M. microti* n=11) archived FFPE (muco)cutaneous and lymph node biopsies of tuberculous lesions were selected; they came from throughout England and Scotland. Further details are available in Table 1.

Nearly 60% (13/22) of the cats in this study were male, and all cats were neutered. The median age of cats infected with *M. bovis* was 5 years, 1 month, compared to 7 years, 0 months for *M. microti*-infected cats; this difference in age was not statistically significant [P=0.326, odds ratio (OR)=0.99 (0.97 to 1.01)]. Eighty-six percent of cats (19/22) were either domestic short or long-haired cats. Other than case 1, all cats were reported as being hunters, or having outdoor access. Case 1 was an indoor-only cat with no reported contact with potentially infected wildlife; however, it was fed the commercial raw food diet associated with the outbreak of *M. bovis* in cats in England and Scotland in 2018 to 2019 (O'Halloran *et al*. 2019). Infection with FeLV or FIV was not identified in the five cats that were tested.

Table 1. Summary of animal details included in this study

Case	Diagnosis	Method	Age	Gender	Breed	Location	FeLV antigen	FIV antibody	Site of Lesion
1	*M. bovis*	Culture	1 year 0 month	MN	Persian	Greater Manchester	NP	NP	Mesenteric LN
2	*M. bovis*	Culture	1 year 7 months	FN	DSH	Bristol	NP	NP	Mesenteric LN
3	*M. bovis*	Culture	1 year 11 months	FN	DSH	Bristol	NP	NP	Inguinal mass
4	*M. bovis*	Culture	3 years 0 month	FN	DSH	Shropshire	Negative	Negative	Popliteal LN
5	*M. bovis*	Culture	4 years 0 month	MN	DSH	Wiltshire	NP	NP	Submandibular LN
6	*M. bovis*	PCR	5 years 1 month	FN	DSH	East Sussex	NP	NP	Axillary mass
7	*M. bovis*	Culture	5 years 4 months	MN	DSH	Bristol	NP	NP	Flank mass
8	*M. bovis*	Culture	7 years 0 month	FN	DSH	Dorset	NP	NP	Sinonasal mass
9	*M. bovis*	PCR	8 years 0 month	FN	DSH	Somerset	NP	NP	Pedal mass
10	*M. bovis*	Culture	10 years 3 months	MN	DLH	Staffordshire	NP	NP	Inguinal mass
11	*M. bovis*	IGRA	12 years 1 month	MN	DSH	Shropshire	Negative	Negative	Popliteal LN
12	*M. microti*	Culture	1 year 5 months	MN	DSH	Essex	Negative	Negative	Gingival mass
13	*M. microti*	IGRA	2 years 0 month	MN	DSH	Fife	NP	NP	LN (unspecified)
14	*M. microti*	IGRA	5 years 4 months	MN	DSH	Angus	NP	NP	Forelimb mass
15	*M. microti*	IGRA	6 years 6 months	FN	DSH	Perth & Kinross	NP	NP	Leg mass
16	*M. microti*	IGRA	6 years 10 months	FN	DSH	Lancashire	NP	NP	LN (unspecified)
17	*M. microti*	Culture	7 years 0 month	MN	Siamese	London	Negative	Negative	Flank mass
18	*M. microti*	Culture	7 years 0 month	FN	DSH	Angus	NP	NP	Skin (unspecified)
19	*M. microti*	Culture	8 years 0 month	MN	Burmilla	East Lothian	NP	NP	Mesenteric LN
20	*M. microti*	Culture	8 years 0 month	MN	DSH	Kent	NP	NP	Facial mass
21	*M. microti*	Culture	8 years 10 months	MN	DSH	Devon	NP	NP	Facial mass
22	*M. microti*	IGRA	15 years 0 month	MN	DSH	Kent	Negative	Negative	Dorsal mass

PCR Polymerase chain reaction, IGRA Interferon-gamma release assay, MN Male neutered, FN Female neutered, DSH Domestic shorthair, DLH Domestic longhair, FeLV Feline leukaemia virus, FIV Feline immunodeficiency virus, NP Not performed, LN Lymph node
Cats were tested for FeLV p27 antigen and FIV anti-p24 antibodies using the SNAP FIV/FeLV Combo Test, Idexx

Histopathological classification

Summarised results of histological and IHC analysis are presented in Table 2. Results of univariate analysis are reported in Table 3.

The lesions were granulomatous or pyogranulomatous, with macrophages as the predominant cell type in all cases, which were mostly epithelioid. Neutrophils were often present and were either dispersed throughout the lesion or accumulated in areas of necrosis. Lymphocytes were less frequently identified and were often located towards the periphery of lesions. Multinucleated giant cells were not identified in any sample.

A proportion of lesions of both aetiologies (10/22) were similar in appearance to typical tuberculous granulomas (Martin *et al.* 2016, Pagán & Ramakrishnan 2018), and these were termed "*organised*" granulomas (Fig 1A, B). "Organised" lesions had singular or multifocal zones of central caseous necrosis, surrounded by a layer of macrophages and epithelioid macrophages; neutrophils were also a common feature within this cell layer. Lymphocytes and plasma cells, where present, were often located towards the periphery of the lesions, and/or less often distributed throughout the lesion (where they occasionally clustered). There was inter-individual variation in lesion encapsulation, and an outer layer of concentrically arranged spindle-shaped cells admixed with eosinophilic fibrillary material (fibrous capsule), which ranged from a thick capsule surrounding the entire granuloma to no encapsulation at all. Where no obvious capsule was present, the inflammatory infiltrate extended into surrounding tissue.

The remaining lesions (12/22) had minimal to absent central necrosis. Clusters of epithelioid and non-epithelioid macrophages were present, with interspersed neutrophils and variable numbers of lymphocytes. These lesions were termed "*atypical*" granulomas (Fig 1C, D). Importantly, "atypical" lesions presented with well defined, mostly round, small epithelioid macrophage clusters (100 µm-1000 µm), often divided by thin fibrous septa into smaller clusters, with very rare and mild central necrosis. The presence of a well-defined outer fibrous capsule was variable, as for "organised" lesions.

Both granuloma types effaced and expanded pre-existing tissue and presented with frequent areas of collagen degeneration with increased intercellular spacing (oedema), with or without inflammation, as well as variable demarcation.

Eight of 11 *M. bovis*-associated lesions were classified as "organised," compared with two of 11 *M. microti*-associated lesions; the remaining three and nine lesions were deemed "atypical" for each aetiology, respectively. There was a statistically significant difference between aetiology and granuloma type in univariate logistic regression [P=0.024, OR=0.08 (0.01 to 0.73)], with "organised" lesions being more likely to arise from infection with *M. bovis*.

Necrosis and fibrosis

Necrosis, as defined previously, was identified in 11 of the 22 cases examined, with larger necrotic areas in lesions with "organised" granulomas (these lesions had central necrosis, as described above). Most "atypical" tuberculous granulomas did not have any central necrosis, but clusters of necrotic neutrophils were identified in case 20 (Fig 1E). The median percentage area of necrosis

Table 2. Summarised details of histological and immunohistochemical analysis of feline tuberculous lesions

Case	Aetiology	Granuloma t-ype	Average AFB/hpf	BI score	BI grade	% Necrosis	% Fibrosis	% Calprotectin	% CD3	% Pax5
1	*M. bovis*	"Organised"	63.40	4	H	50.8	28.3	20.5	0.1	<0.1
2	*M. bovis*	"Organised"	22.20	4	H	58.9	1.2	5.6	0.4	<0.1
3	*M. bovis*	"Atypical"	8.87	3	H	0.0	46.6	13.5	0.1	<0.1
4	*M. bovis*	"Organised"	0.53	2	L	18.3	0.7	30.0	3.2	0.2
5	*M. bovis*	"Organised"	5.47	3	H	51.3	3.2	9.7	0.2	0.1
6	*M. bovis*	"Organised"	34.40	4	H	18.4	1.0	19.1	6.7	0.6
7	*M. bovis*	"Atypical"	0.93	2	L	0.0	23.8	22.2	8.5	0.3
8	*M. bovis*	"Organised"	0.33	2	L	6.9	10.5	10.4	0.8	0.1
9	*M. bovis*	"Organised"	11.47	4	H	27.0	8.5	16.1	4.3	0.8
10	*M. bovis*	"Organised"	15.60	4	H	32.0	33.8	14.2	8.4	0.5
11	*M. bovis*	"Atypical"	0.07	1	L	0.0	16.2	13.8	5.7	0.4
12	*M. microti*	"Atypical"	172.93	5	H	0.0	2.5	8.7	1.6	0.2
13	*M. microti*	"Atypical"	0.00	0	L	0.0	1.1	15.9	0.6	<0.1
14	*M. microti*	"Organised"	0.47	2	L	28.4	35.5	32.2	1.7	<0.1
15	*M. microti*	"Atypical"	0.27	2	L	0.0	8.8	9.7	0.3	0.1
16	*M. microti*	"Atypical"	0.00	0	L	0.0	13.2	3.9	1.3	<0.1
17	*M. microti*	"Atypical"	1.40	3	H	0.0	12.9	28.1	6.9	0.7
18	*M. microti*	"Atypical"	0.33	2	L	0.0	10.0	12.1	6.5	0.1
19	*M. microti*	"Atypical"	0.07	1	L	0.0	4.6	11.1	0.3	<0.1
20	*M. microti*	"Atypical"	0.20	2	L	9.3	3.8	18.8	1.3	0.1
21	*M. microti*	"Organised"	42.60	4	H	8.6	24.3	11.7	10.3	0.7
22	*M. microti*	"Atypical"	0.27	2	L	0.0	31.0	21.7	0.2	0.1

AFB Acid-fast bacilli, hpf High power field, BI Bacterial index, H High, L Low

Granuloma type was classified as either "organised" or "atypical." "Organised" granulomas consisted of a central necrotic core surrounded bey a cellular layer composed of epithelioid macrophages, macrophages and neutrophils. "Atypical" granulomas lacked a central necrotic core and consisted of tight aggregates of epithelioid macrophages, macrophages and neutrophils. In both granuloma types, lymphocytes were predominantly located at the periphery of the granuloma, and there was variable deposition of collagen fibres forming an external capsule in "organised" granulomas, or thin fibrous septa in "atypical" granulomas. "% Necrosis" and "% Fibrosis" is the area of each histological feature relative to the total area of the lesion, as determined on Haematoxylin & Eosin-, and Masson's Trichrome-stained slides. "% Calprotectin," "% CD3" and "% Pax5" is the area of positive staining for each marker relative to the total area of the lesion. Positive staining for calprotectin indicates the presence of granulocytes and recently blood-derived monocytes, CD3 for T-lymphocytes and Pax5 for B-lymphocytes

Table 3. Results of univariate binomial logistic regression analysis

Variable	Summary statistics [median (range)]		Odds ratio	95% CI	P-value
	M. bovis	*M. microti*			
Granuloma type	A: 3, O: 8	A: 9, O: 2	0.08	0.01 to 0.73	0.024
Necrosis	18.42% (0.00 to 58.90%)	0.00% (0.00 to 28.35%)			
0.00%	3	8	Baseline	—	—
0.01 to 10%	3	2	3.76	0.30 to 47.16	0.305
>10%	5	1	17.11	1.09 to 268.31	0.043
BI category	H: 7, L: 4	H: 3, L: 8	0.14	0.01 to 1.35	0.088
Pax5	0.16% (<0.01 to 0.83%)	0.07% (<0.01 to 0.72%)			
0.00 to 0.09%	4	6	Baseline	—	—
0.10 to 0.50%	4	3	4.46	0.36 to 54.83	0.243
>0.50%	3	2	8.91	0.35 to 228.43	0.186
Gender	MN: 5, FN: 6	MN: 8, FN: 3	0.31	0.05 to 1.85	0.200
Fibrosis	10.54% (0.69 to 46.57%)	9.95% (1.12 to 35.46%)			
0.00 to 10%	5	6	Baseline	—	—
10.01 to 20%	2	2	2.00	0.13 to 31.62	0.623
20.01 to 30%	2	1	7.64	0.31 to 187.52	0.213
>30%	2	2	4.48	0.19 to 106.37	0.353
Calprotectin	14.15% (5.57 to 30.05%)	12.09% (3.91 to 32.15%)			
0.00 to 10%	2	3			
10.01 to 20%	6	5	3.78	0.35 to 45.14	0.294
>20%	3	3	3.96	0.22 to 71.26	0.350
Age	5y 1m (1y 0m to 12y 1m)	7y 0m (1y 5m to 15y 0m)	0.99	0.97 to 1.01	0.326
CD3	3.20% (0.07 to 8.49%)	1.30% (0.17 to 10.32%)			
0.00 to 1%	5	4	Baseline	—	—
1.01 to 5%	2	4	0.36	0.03 to 3.88	0.402
>5%	4	3	2.25	0.18 to 27.65	0.528
Tissue	Skin: 6, LN: 5	Skin: 8, LN: 3	0.69	0.12 to 3.78	0.665

BI Bacterial Index, A "Atypical", O "Organised", H High, L Low, MN Male neutered, FN Female neutered, y Years, m Months, LN Lymph node, CI Confidence interval
Age, gender and tissue were included as covariates for univariate regression of Necrosis, BI Category, Pax5, Calprotectin and CD3. Necrosis, Pax5, Calprotectin and CD3 P-values were calculated using the lowest group classification as the reference group. Goodness-of-fit analysis showed insufficient evidence to conclude the models did not fit the data (data not shown)

within *M. bovis* lesions was 18.3% (0.0 to 59.8%), compared to 0.0% (0.0 to 28.3%) for *M. microti* lesions. This was reflected in the results of univariate logistic regression, where if more than 10% of the lesion consisted of necrotic tissue, *M. bovis* was significantly more likely to be the organism associated with the lesion [P=0.043, OR=17.11 (1.09 to 268.31)].

In terms of fibrosis, there appeared to be qualitative differences in the distribution of collagen fibres within feline TB lesions; *M. bovis* lesions showed thicker bands of collagen fibres surrounding larger "organised" granulomas, whereas *M. microti* lesions displayed thinner fibrous septa dividing smaller "atypical" granulomas (Fig 1F). However, the total proportion of the lesion occupied by collagen fibres did not differ between aetiologies in univariate analysis (P > 0.213).

Acid-fast bacilli counts and bacterial index category

AFB were identified in the ZN-stained section on examination of 15 hpf in 91% (20/22) of the samples. For the remaining two samples, the entire slide was examined to look for AFB; a single ZN-positive organism morphologically consistent with mycobacteria was identified in case 16, whereas no AFB were identified in case 13. Fifty-five percent of specimens scored as low BI (12/22); there was no statistical difference between the number of *M. bovis* and *M. microti* lesions scoring as low BI (P=0.088, OR=0.14 [0.01 to 1.35]). These data underline the variability in the number of organisms seen in feline tuberculosis lesions (*M. bovis* median: 8.87, range: 0.07 to 63.40; *M. microti* median: 0.27, range: 0.00 to 172.93). Case 12 scored BI 5, displaying vast numbers of AFB (Fig 2), often with an S-shaped morphology, and there were x1000 microscope fields from five other cats (cases 1, 2, 6, 9 and 21) with over 100 AFB (data not shown). ZN-positive organisms were found both intra- and extracellularly. Extracellular AFB were often located within areas of necrosis for both pathogens.

Calprotectin immunohistochemistry

Calprotectin-positive cells, *i.e.* granulocytes, monocytes and recently blood-derived macrophages, with strong granular to diffuse cytoplasmic staining were present in all samples; for each case calprotectin had more percentage-lesion positive immunolabelling than CD3 and Pax5. In lesions with large areas of necrosis, calprotectin-positive cells were common at the cell-necrosis interface, throughout the necrosis and within the regions of (pyo) granulomatous inflammation (Fig 3A, B). Cells morphologically consistent with macrophages and neutrophils were positive for calprotectin, while epithelioid macrophages were negative. Necrotic regions showed variable amounts of positive staining which was not associated with intact cells or tissue; where appropriate, these areas were removed from image analysis when quantifying the total area of cell-specific calprotectin-positive immunolabelling. Differences in calprotectin expression did not infer infection between the pathogens in univariate analysis (P > 0.294).

CD3 immunohistochemistry

Cells with moderate to strong membranous staining for CD3 (*i.e.* T-lymphocytes) were the second most common cell population

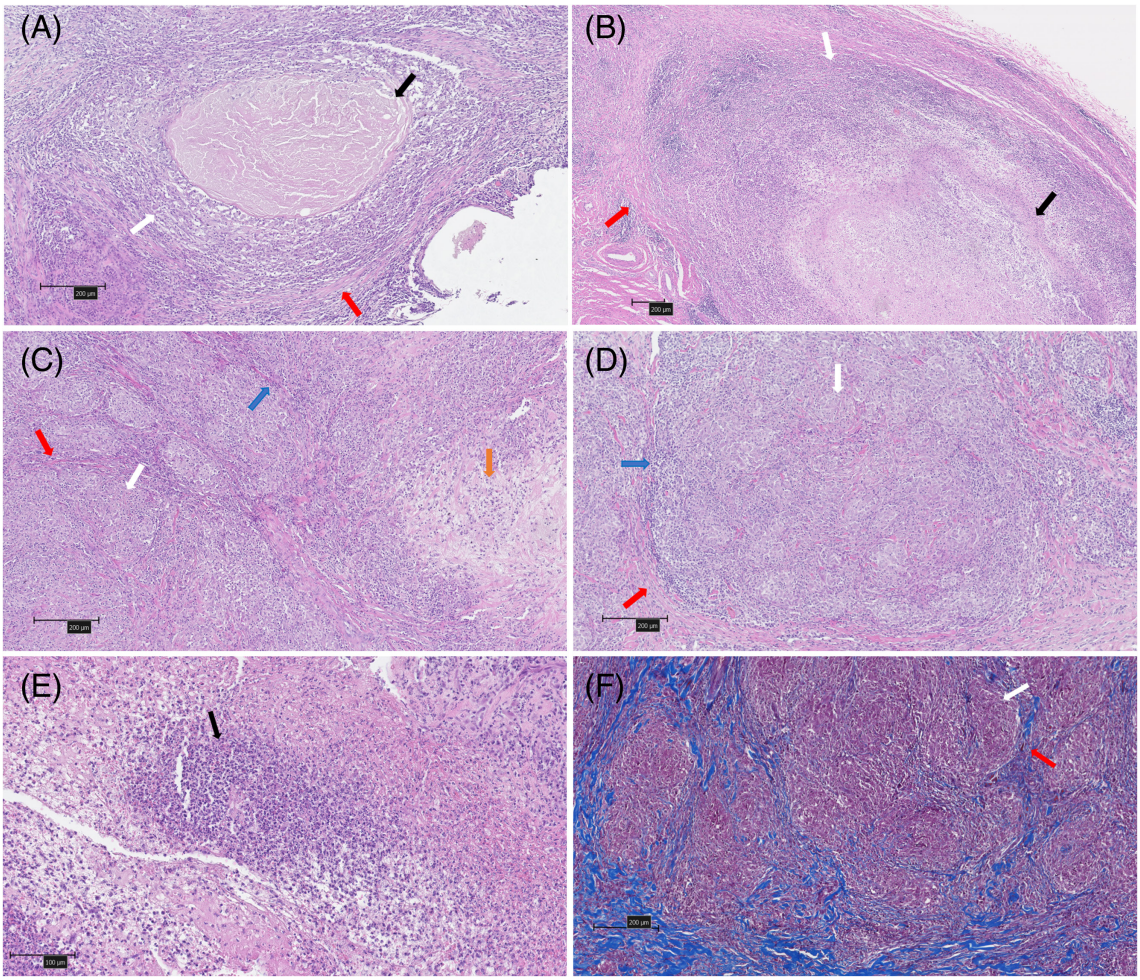

FIG 1. Representative images of H&E (A-E) and Masson's Trichrome (F) stained feline tuberculosis lesions; "organised" granuloma, *M. bovis* (A, top left) with central necrosis (black arrow), macrophage and neutrophil cell layer (white arrow) and incomplete fibrous encapsulation (red arrow), magnification ×10, scale bar 200 μm; "organised" granuloma, *M. microti* (B, top right) showing a necrotic centre (black arrow) with a pyogranulomatous cellular layer (white arrow) and a thick fibrous capsule (red arrow), ×5, scale bar 200 μm; "atypical" granuloma, *M. bovis* (C, centre left) featuring small clusters of macrophages and some neutrophils (white arrows), with peripherally located lymphocytes (blue arrow) divided by fibrous septa (red arrows), with areas of degenerating collagen, oedema, and a mixed inflammatory cell population (orange arrow), magnification ×10, scale bar 200 μm; "atypical" granuloma, *M. microti* (D, middle right) displaying clusters of macrophages and neutrophils (white arrows), a peripheral zone of lymphocytes (blue arrow) and thin fibrous encapsulation (red arrow), ×10, scale bar 200 μm; "atypical" granuloma, *M. microti* (E, bottom left) cluster of necrotic neutrophils (black arrow), ×20, scale bar 100 μm; "atypical" granuloma, *M. microti* (F, bottom right) demonstrating the thin fibrous incomplete encapsulation (red arrow) around clusters of macrophages and neutrophils (white arrow), magnification ×10, scale bar 200 μm

identified. They were located peripherally and scattered throughout all lesions (Fig 3C). The percentage-lesion positive staining for CD3 was not statistically significant different between the pathogens in univariate analysis ($P > 0.402$).

Pax5 immunohistochemistry

Strong, diffuse nuclear staining for Pax5 was seen in cells towards the periphery of lesions. These B-cells were sometimes observed in clusters (Fig 3D). The total area of positive staining for Pax5 did not exceed 1% in any section, and there was comparatively greater staining of CD3 than Pax5 for each case (Table 2). Pax5 percentage-lesion positive staining did not differ between the pathogens, although the statistical significance when Pax5 positivity exceeded 0.50% was met for inclusion in multivariate analysis [P=0.186, OR=8.91 (0.35 to 228.43)], based on the *a priori* threshold for significance on univariate analysis of $P < 0.20$.

Multivariate analysis

"Organised" vs "atypical" granulomas, amount of necrosis, BI category, Pax5 positive staining and gender were identified from univariate analysis for inclusion in a multivariate model. Age and tissue were also included as covariates. Preliminary exploration of the data showed that necrosis was highly collinear with granuloma type and was therefore excluded from multivariate modelling. The results of the final multivariate model identified no statistically significant factors suggesting infection with either *M. bovis* or *M. microti* (Table 4); granuloma type appeared to be the most important factor in this model [P=0.074, OR=0.01 (0.00005 to 1.52)], with *M. bovis* lesions being more likely to show "organised" granuloma morphology. The generalised variance inflation factor (GVIF) for all variables was calculated and normalised by the degrees of freedom; the corrected GVIF did not exceed 2.35 for any variable. A multidirectional stepwise algorithm was run

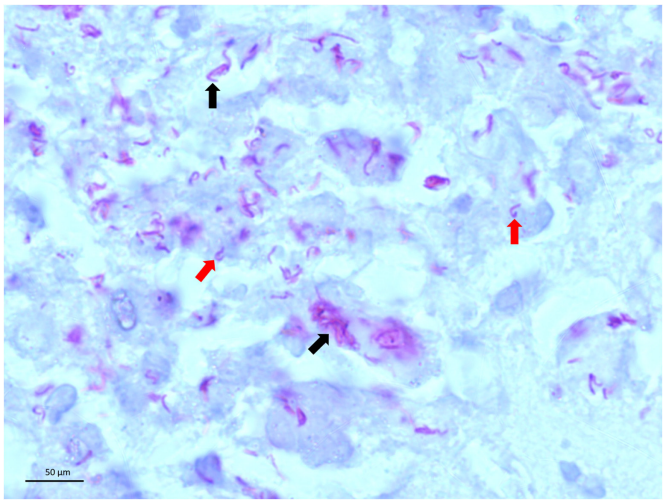

FIG 2. Numerous intracellular acid-fast bacilli present in clusters (black arrows) or individually (red arrows) on Ziehl-Neelsen staining in a case of *Mycobacterium microti* infection (Case 12). This sample was scored as Bacterial Index 5. Note the characteristic S-shaped bacteria, ×1000. Scale bar 50 µm

to identify the simplest model that could infer infection with either *M. bovis* or *M. microti*; this suggested a model with "organised" vs "atypical" granulomas as the only significant predictor for aetiology [P=0.016, OR=0.08 (0.01 to 0.63)].

DISCUSSION

This study described and compared feline tuberculous lesions, using histology and IHC to identify potential features that could infer infection with either *M. bovis* or *M. microti* histologically at an early stage of the diagnostic investigation.

Among the companion animal population, the domestic cat appears to be much more susceptible to mycobacterial infections than other species, such as dogs (Broughan *et al.* 2013), and when outbreaks of disease do occur they can be devastating (O'Halloran *et al.* 2019). The role of companion animal species in the epidemiology of bovine TB in the UK is controversial; it has been shown that cats can become infected with the same *M. bovis* spoligotypes and genotypes as cattle (Monies *et al.* 2000, Gunn-Moore *et al.* 2011a), and endemic *M. microti* infection may provide a degree of protection against *M. bovis* infection (Smith *et al.* 2009). Others argue that cats most likely represent spill-over hosts for mycobacterial infections (Broughan *et al.* 2013). However, the high prevalence of TB in cats, particularly *M. bovis* infection (Gunn-Moore *et al.* 2011a), poses a real zoonotic risk to owners and the veterinary staff who handle and care for these animals (O'Connor *et al.* 2019). Both *M. bovis* and *M. microti* are capable of infecting cats and causing clinical disease. Differentiating between these two pathogens can be complicated, although the geographical location can suggest which is most likely (Gunn-Moore *et al.* 2011a). The reference standard diagnostic test is specialist mycobacterial culture, however, its sensitivity is only approximately 50%, and while more rapid diagnostic tests are available, they are non-validated and also have their limitations (Gunn-Moore 2014). The need for more commercially available and financially viable diagnostics for mycobacterial disease in cats is therefore imperative.

The median age of cats infected with *M. bovis* in the current study was higher than previously reported, whereas the age of *M. microti*-infected cats was similar (Gunn-Moore *et al.* 2011a). Neutered male cats with outdoor access were the largest demographic in the current study. Additionally, 19 of 22 cats were domestic short- or long-haired, consistent with previous findings (Gunn-Moore *et al.* 2011a). The single cat not reported to have outdoor access had been fed a commercially available raw food diet, that was previously implicated as the likely cause of an outbreak of *M. bovis* in predominantly indoor, pure-breed cats (O'Halloran *et al.* 2019).

The histopathological features of feline *M. bovis* and *M. microti* lesions has not been directly compared previously, and in this study, *M. bovis* lesions were more frequently classified as "organised" granulomas, with structural similarities to typical tuberculous granulomas observed in other species, *i.e.* a central necrotic core with a macrophage-dominant cellular layer and an outer rim of lymphocytes, with or without an external fibrous capsule (Pagán & Ramakrishnan 2018). In contrast with these descriptions, feline *M. bovis*-associated lesions often had abundant neutrophils present within zones of granulomatous inflammation, lacked MNGCs and did not show evidence of mineralisation. Conversely, lesions from cats infected with *M. microti* were more often composed of tightly packed, smaller macrophage clusters with or without neutrophils. These lacked a necrotic core in most cases, and were delimited by intermittent, thin capsules. To differentiate these from the previous presentation they were termed "atypical" granulomas.

These histopathological differences in the arrangement, organisation and structure of granulomas may be due to the host immune response to infection. Studies into the serum cytokine and chemokine profile of cats infected with mycobacteria show increased concentrations of tumour necrosis factor alpha (TNFα) in cats infected with *M. bovis* compared to those infected with *M. microti* (O'Halloran *et al.* 2018). TNFα is a potent pro-inflammatory cytokine, secreted primarily by monocytes, macrophages and dendritic cells (Van Crevel *et al.* 2002), and it plays an important role in the host immune response to mycobacterial infections through activating macrophages to promote phagocytosis and subsequent killing of mycobacteria, inducing expression of chemokines by macrophages resulting in the recruitment of $CD4^+$ T-lymphocytes, driving necrosis of infected macrophages, and the formation and maintenance of granulomas (Laster *et al.* 1988, Flynn *et al.* 1995, Roach *et al.* 2002, O'Garra *et al.* 2013, Dorhoi & Kaufmann 2014). It also has been shown to stimulate fibroblasts (Battegay *et al.* 1995), which may contribute to the deposition of collagen fibres to encapsulate granulomas. However, excessive TNFα may result in disruption of normal granuloma formation, with overactivation of macrophages resulting in increased necrosis with release of intracellular mycobacteria into the necrotic milieu (Dorhoi & Kaufmann 2014). Conversely, cats with *M. microti* showed increased levels of platelet-derived growth factor-BB (PDGF-BB), which is a potent mitogen of

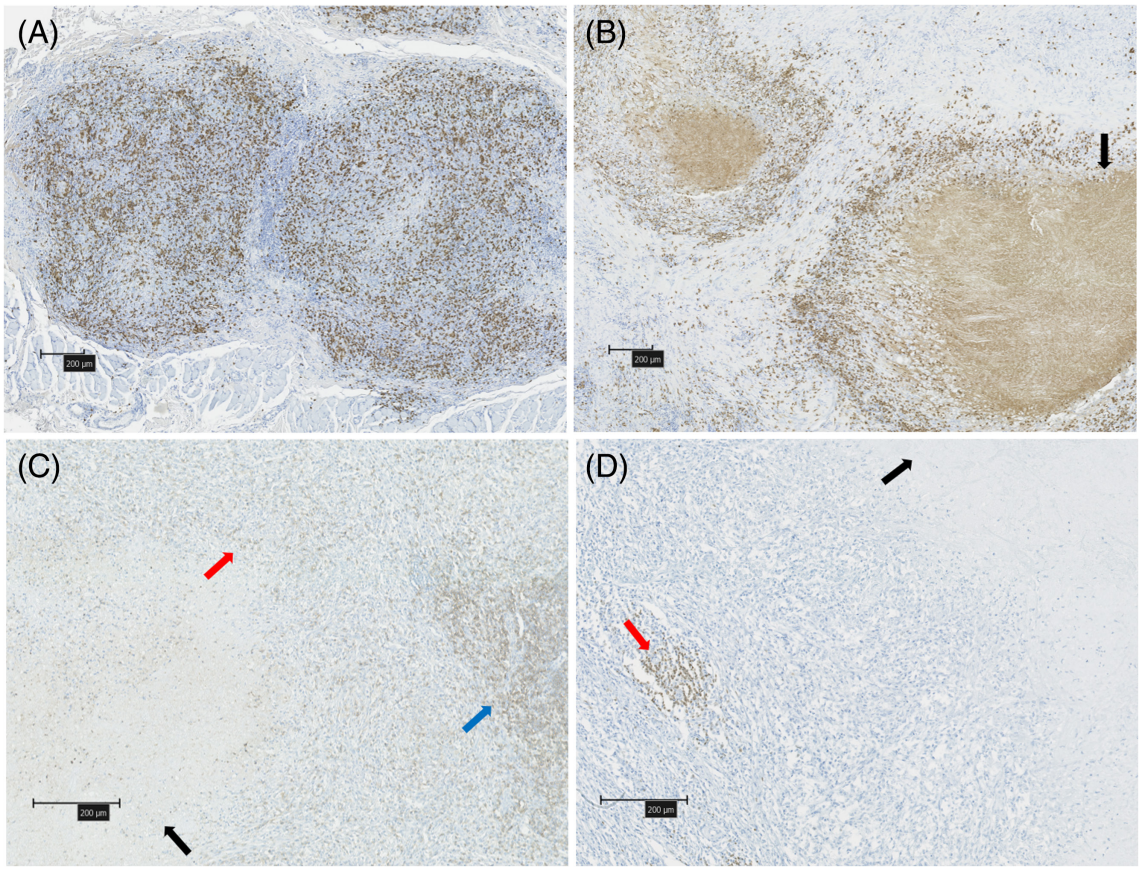

FIG 3. Immunohistochemistry of feline tuberculosis lesions to assess (A) calprotectin expression, ×5; (B) calprotectin expression in regions of necrosis (black arrow), ×5; (C) CD3 expression in a tuberculous lymph node lesion (red arrow) and effaced remnants of paracortical lymph node tissue (blue arrow), with minimal CD3-positive cells in regions of necrosis (black arrow) ×10; (D) expression of Pax5 in a subcutaneous tuberculous lesion (red arrow), with no positive staining cells in necrotic regions (black arrow), ×10. Scale bar 200 μm

Table 4. Results of multivariate logistic regression, modelling factors where P <0.20 on univariate analysis

Variable	Summary statistics [median (range)]		Odds ratio	95% CI	P-value
	M. bovis	*M. microti*			
Overall	—	—	—	—	0.113
Structure	A: 3, O: 8	A: 9, O: 2	0.08	0.00005 to 1.52	0.074
Pax5	0.16% (<0.01 to 0.83%)	0.07% (<0.01 to 0.72%)			
0.00 to 0.09%	4	6	Baseline	—	—
0.10 to 0.50%	4	3	18.94	0.46 to 788.00	0.122
>0.50%	3	2	0.02	0.00001 to 42.10	0.323
Gender	MN: 5, FN: 6	MN: 8, FN: 3	0.08	0.003 to 2.30	0.144
BI category	L: 4, H: 7	L: 8, H: 3	0.02	0.00005 to 4.56	0.150
Age	5y 1m (1y 0m to 12y 1m)	7y 0m (1y 5m to 15y 0m)	1.02	0.97 to 1.09	0.364
Tissue	Skin: 6, LN: 5	Skin: 8, LN: 3	0.31	0.01 to 9.31	0.507

BI Bacterial Index, A "Atypical", O "Organised", MN Male neutered, FN Female neutered, L Low, H High, y Years, m Months, LN Llymph node, CI Confidence interval
The data are adequately described by the model (Hosmer-Lemeshow goodness of fit, P=0.235)

fibroblasts and plays an important role in fibroblast proliferation and deposition of collagen (Agren *et al.* 1999, Van Der Kroef *et al.* 2020). It has also been shown that PDGF-BB enhances TNFα-induced chemokine secretion by fibroblasts and production of collagen (Van Der Kroef *et al.* 2020). The increased levels of TNFα in cats with *M. bovis*-infection may contribute to more necrosis within lesions, while increased PDGF-BB in *M. microti*-infected cats may result in differences in the pattern of collagen deposition, resulting in smaller granulomas divided by fibrous septa. Differences in the chronicity of the lesion may also play a role, with increased deposition of collagen as lesions progress and become more chronic as reported for cattle (Wangoo *et al.* 2005). However, due to the clinical nature of the submitted samples it is unknown how long the lesions had been present or when infection occurred. It is therefore not possible to classify samples according to age or know how long the lesions had to develop the structural organisation of the (pyo)granulomatous infiltrate observed. It is possible that the variability in the presentation

stems from the bacteria themselves, and one can hypothesise that these histological differences could be mediated by key virulence factors. It has been shown that ESAT-6 is a leucocidin resulting in neutrophil necrosis (Francis *et al*. 2014); this virulence factor may contribute to the increased amount of necrosis in *M. bovis*-associated lesions. Furthermore, granuloma type and macrophage aggregation is disrupted following infection with RD1 mutant mycobacteria in an experimental setting (Volkman *et al*. 2004, Davis & Ramakrishnan 2009); the lesions described in this study from cats with *M. microti* infection, which can be thought of as a natural RD1 deletion mutant (Frota *et al*. 2004), would appear to support this finding that RD1 proteins play a role in the structure and organisation of mycobacterial granulomas.

AFB were present in 91% of the lesions examined in the current study, in contrast with previous studies which reported that ZN-positive organisms morphologically consistent with mycobacteria were identified in only approximately 30% (37/134) of feline mycobacterial histopathological samples (Gunn-Moore *et al*. 2013). As has been previously reported, *M. microti* AFB often presented with an S-shaped morphology (Van Soolingen *et al*. 1998). It is of note that identification of AFB can be analyst dependent (Gunn-Moore *et al*. 2011b), and mycobacteria can alter their cell wall composition, resulting in a loss of "acid-fastness" on ZN staining (Seiler *et al*. 2003). Application of the BI scoring system when reporting on ZN-staining of diagnostic samples is recommended for future studies, as it enables more consistent reporting compared to subjective terms to describe the number of ZN-positive organisms present. For example, this is likely to provide a robust reference in the comparative assessment of diagnostic tests, *e.g*. the likelihood of obtaining a positive PCR result on FFPE tissues with differing BI scores. Of interest, 45% (10/22) of samples had a high BI in this study, and one *M. microti* sample even scored as grade 5 (100.01 to 1000 AFB/hpf). This finding is directly relevant for diagnostics, as feline TB is often thought of as a paucibacillary infection, while multibacillary lesions typically indicate infection with non-tuberculous, and therefore non-zoonotic, mycobacterial species (Davies *et al*. 2006). The data presented here show that feline MTBC infections can present with abundant AFB, so discriminating between TB and NTM infections based on the number of AFB and BI scoring is not possible.

This study did not identify differences between the area of calprotectin-positivity in *M. bovis* and *M. microti* lesions. Calprotectin is expressed by circulating monocytes and those freshly recruited to developing areas of (pyo)granulomatous inflammation, plus granulocytes and some subsets of activated macrophages (Zwadlo *et al*. 1986). As monocytes differentiate into macrophages there is a loss of calprotectin expression, whereas expression of CD163 is upregulated (Zwadlo *et al*. 1985). The high proportion of lesions expressing calprotectin suggests active development of the inflammatory infiltrate, with ongoing recruitment of monocytes and neutrophils (Rugtveit *et al*. 1996). Many macrophages, notably those with an epithelioid phenotype, did not express this molecule, suggesting differentiation and subsequent loss of calprotectin expression; this is consistent with what has been previously reported in cases of feline mycobacteriosis (Kipar *et al*. 2003). The proportion of calprotectin-positive cells has been shown to decrease in more chronic tuberculous granulomas in other species (García-Jiménez *et al*. 2012, García-Jiménez *et al*. 2013), therefore the tissues in this study with lower levels of calprotectin expression could reflect the presence of more chronic lesions. While identification of calprotectin-positive cells can give an insight to the active recruitment of monocytes and granulocytes to the granuloma, it does not fully characterise the macrophage cell populations present, which is a limitation of this study. Alternative pan-macrophage markers, such as ionised calcium-binding adapter molecule 1 (Iba1), may be more specific for detection of macrophage populations within tuberculous lesions (Pierezan *et al*. 2014), while staining for CD163 could identify anti-inflammatory M2 macrophage populations (McBride *et al*. 2017). Additionally, markers such as Ki-67 could be used to identify local macrophage proliferation (McBride *et al*. 2017), providing further description of these lesions above what can be achieved by staining for calprotectin alone.

No differences were observed between *M. bovis* and *M. microti* lesions regarding positivity for T- or B-lymphocyte markers. Both T- and B-lymphocytes were located peripherally in tuberculous lesions in the current study and were a minor component of the inflammatory infiltrate. For each cat, the area of positive staining for T-lymphocytes exceeded that for B-lymphocytes, suggesting T-lymphocytes may play a greater role to the composition of the granuloma and to the pathogenesis of feline MTBC infections. In other species, T-lymphocytes expressing CD3 appear to be present within tuberculous lesions at consistent levels across different stages of granuloma development (García-Jiménez *et al*. 2013, Salguero *et al*. 2017). The role of T-lymphocytes in the pathogenesis of tuberculous infections, characteristic of a type IV hypersensitivity response, has been well studied and reviewed (Schluger & Rom 1998, O'Garra *et al*. 2013); $CD4^+$ lymphocytes, and in particular T-helper 1 cells, play an important role in developing protective immunity against mycobacteria as well as stimulating macrophage activity via secretion of IFNγ. $CD4^+$-deficient individuals have been shown to be more susceptible to mycobacterial infections (Geldmacher *et al*. 2008), and idiopathic $CD4^+$ lymphocytopenia has been documented in a cat with disseminated *M. xenopi* infection (Meeks *et al*. 2008). The role of other T-cell subsets, including CD8+ and $\gamma\delta$ TCR+ T-cells, are less well elucidated (Schluger & Rom 1998), although it has been suggested that $\gamma\delta$ T-cells may play an important role in the pathogenesis of bovine mycobacterial infections (Guzman *et al*. 2012). The proportion of B-lymphocytes expressing CD20 or CD79a, appears to increase in some species (García-Jiménez *et al*. 2012, Vallejo *et al*. 2018), possibly indicating a shift towards humoral immunity as the disease progresses. The role of B-lymphocytes in the pathogenesis of TB has been often overlooked, although there is gathering evidence that B-lymphocytes may interact with and regulate the response of T-lymphocytes in chronic infections, in addition to driving differentiation of alternatively-activated M2 macrophages, which play a modulatory role in mycobacterial infections (Martinez & Gordon 2014). Plasma cells, which were rarely identified on H&E-stained sections, do not express Pax5 (Barberis *et al*. 1990, Feldman & Dogan 2007), so they were not

identified by IHC in this study; their contribution to tuberculous lesions in cats could be explored further through use of markers such as immunoglobulin λ light-chain (Mellor *et al*. 2008). However, the results of the current study appear consistent with findings observed in tuberculous lesions in other species (Kipar *et al*. 2003, García-Jiménez *et al*. 2013).

Tuberculosis affects a wide range of organs and body systems, but histological and immunological studies have normally been performed on lung or lymph node granulomas (Turner *et al*. 2003, Wangoo *et al*. 2005, García-Jiménez *et al*. 2012, García-Jiménez *et al*. 2013); since feline tuberculous lesions are predominantly cutaneous, this may explain why previously established granuloma scoring systems did not correspond well to feline lesions. A review of cutaneous mycobacterial lesions in humans identified seven different histopathological patterns, including "organised" tuberculoid granulomas, but it was also noted that multiple patterns could be present within the same biopsy sample examined and that the histopathological presentation of disease could not classify infection with different mycobacterial species (Santa Cruz & Strayer 1982). Neutrophils also appeared to be more frequently identified in cutaneous mycobacterial lesions (Santa Cruz & Strayer 1982). Differences in host-pathogen interactions between host species have also been identified; human *M. tuberculosis* infection typically results in the formation of caseous granulomas, whereas non-necrotic lesions are more common in some strains of mice (Kramnik *et al*. 2000). Similarly, *M. microti* infection in its maintenance host, the field vole, often results in caseous necrosis with associated regions of dystrophic mineralisation, and MNGCs (Kipar *et al*. 2014), features which were mostly absent from feline lesions. Studies into the histological and immunological appearance of mycobacterial lesions affecting other organs, such as the eye, could provide further insights as to whether lesion development varies due to the tissue or organ infected, the infecting organisms present, or whether the feline immune response differs compared to that in other species. As this study used clinical cases of naturally occurring TB, managed by referring veterinarians, data such as the chronicity of lesions and the duration of formalin-fixation of the sample was unavailable, so it is not possible to exclude that some of the histological and immunological differences could be explained by this.

The results of the histological analyses warrant further investigation on a larger set of confirmed tuberculous samples as the small sample size may be insufficient to support a multivariate model. Furthermore, categorising the continuous variables that did not meet the assumptions for binomial logistic regression results in a loss of statistical power and the interpretation of any statistically significant findings is more complicated. Additionally, multicollinearity of some of the variables in this study was identified; where appropriate, collinear variables were excluded from models which were deemed to not result in a loss of biological explanation of the results. Despite the above limitations, in this study the granuloma type was the most statistically significant finding in suggesting whether a cat was infected with *M. bovis* or *M. microti*. This is relevant, as the findings of this study are useful in the diagnostic histopathology setting to infer the likelihood of infection with either *M. bovis* or *M. microti* before further testing, *i.e*. culture, PCR or IGRA.

In conclusion, this study characterised the histological and immunohistochemical appearance of tuberculous lesions in cats naturally infected with *M. bovis* or *M. microti*. With ZN staining, *M. microti* AFB were frequently S-shaped, and numerous AFB were observed in individual cases for both *M. bovis* and *M. microti* infections. Therefore, abundant ZN-positive organisms are not a specific diagnostic feature of feline infection with non-zoonotic NTM species. The study identified differences in the histopathological features between these two mycobacterial species that may raise the index of suspicion for infection with either mycobacterial species at an earlier stage of the clinical investigation of these cases.

Acknowledgements

The authors would like to thank Dr Helen Brown and Dr Darren J Shaw for discussions regarding the statistical analysis, Mr Neil MacIntyre for technical assistance with immunohistochemical protocols, the Veterinary Pathology Unit of The Royal (Dick) School of Veterinary Studies for providing control tissue samples and performing Masson's Trichrome staining and the veterinary staff, owners and pets who have contributed to ongoing research into mycobacterial disease at The University of Edinburgh. This study was supported by funding from BSAVA Petsavers (CRP 03.18). JLM is supported by a Biotechnology and Biological Sciences Research Council (BBSRC) studentship (BB/M010996/1). JCH is funded by BBSRC Institute Strategic Programme funding (BB/P013740/1 and BBS/E/D/20002174).

Conflict of interest

None of the authors of this article has a financial or personal relationship with other people or organisations that could inappropriately influence or bias the content of the paper.

References

Adams, D. O. (1976) The granulomatous inflammatory response: a review. *The American Journal of Pathology* **84**, 164-192

Agostinelli, C., Sabattini, E., Gjørret, J. O., *et al*. (2010) Characterization of a new monoclonal antibody against *Pax5*/BASP in 1525 paraffin-embedded human and animal tissue samples. *Applied Immunohistochemistry & Molecular Morphology* **18**, 561-572

Agren, M. S., Steenfos, H. H., Dabelsteen, S., *et al*. (1999) Proliferation and Mitogenic response to PDGF-BB of fibroblasts isolated from chronic venous leg ulcers is ulcer-age dependent. *Journal of Investigative Dermatology* **112**, 463-469

Aranaz, A., Liébana, E., Pickering, X., *et al*. (1996) Use of polymerase chain reaction in the diagnosis of tuberculosis in cats and dogs. *Veterinary Record* **138**, 276-280

Bankhead, P., Loughrey, M., Fernández, J., *et al*. (2017) QuPath: open source software for digital pathology image analysis. *Scientific Reports* **7**, 16878

Barberis, A., Widenhorn, K., Vitelli, L., *et al*. (1990) A novel B-cell lineage-specific transcription factor present at early but not late stages of differentiation. *Genes & Development* **4**, 849-859

Battegay, E. J., Raines, E. W., Colbert, T., *et al*. (1995) TNF-alpha stimulation of fibroblast proliferation. Dependence on platelet-derived growth factor (PDGF) secretion and alteration of PDGF receptor expression. *The Journal of Immunology* **154**, 6040-6047

Bennett, A. D., Lalor, S., Schwarz, T., *et al*. (2011) Radiographic findings in cats with mycobacterial infections. *Journal of Feline Medicine & Surgery* **13**, 718-724

Boniotti, M. B., Gaffuri, A., Gelmetti, D., *et al*. (2014) Detection and molecular characterization of *Mycobacterium microti* isolates in wild boar from northern Italy. *Journal of Clinical Microbiology* **52**, 2834-2843

Broughan, J. M., Downs, S. H., Crawshaw, T. R., *et al*. (2013) *Mycobacterium bovis* infections in domesticated non-bovine mammalian species. Part 1: review of epidemiology and laboratory submissions in Great Britain 2004-2010. *The Veterinary Journal* **198**, 339-345

Burthe, S., Bennett, M., Kipar, A., *et al*. (2008) Tuberculosis (*Mycobacterium microti*) in wild field vole populations. *Parasitology* **135**, 309-317
Canal, A. M., Pezzone, N., Cataldi, A., *et al*. (2017) Immunohistochemical detection of pro-inflammatory and anti-inflammatory cytokines in granulomas in cattle with natural *Mycobacterium bovis* infection. *Research in Veterinary Science* **110**, 34-39
Canfield, P. J., Day, M. J., Gavier-Widen, D., *et al*. (2002) Immunohistochemical characterization of tuberculous and non-tuberculous lesions in naturally infected European badgers (*Meles meles*). *Journal of Comparative Pathology* **126**, 254-264
Chen, Y., Yu, Q. & Xu, C.-B. (2017) A convenient method for quantifying collagen fibers in atherosclerotic lesions by ImageJ software. *International Journal of Clinical Experimental Medicine* **10**, 14904-14910
Davies, J. L., Sibley, J. A., Myers, S., *et al*. (2006) Histological and genotypical characterization of feline cutaneous mycobacteriosis: a retrospective study of formalin-fixed paraffin-embedded tissues. *Veterinary Dermatology* **17**, 155-162
Davis, J. M. & Ramakrishnan, L. (2009) The role of the granuloma in expansion and dissemination of early Tuberculous infection. *Cell* **136**, 37-49
de la Rua-Domenech, R. (2006) Human *Mycobacterium bovis* infection in the United Kingdom: incidence, risks, control measures and review of the zoonotic aspects of bovine tuberculosis. *Tuberculosis* **86**, 77-109
Dippenaar, A., Parsons, S. D. C., Sampson, S. L., *et al*. (2015) Whole genome sequence analysis of *Mycobacterium suricattae*. *Tuberculosis* **95**, 682-688
Dorhoi, A. & Kaufmann, S. H. E. (2014) Tumor necrosis factor alpha in mycobacterial infection. *Seminars in Immunology* **26**, 203-209
Emmanuel, F. X., Seagar, A.-L., Doig, C., *et al*. (2007) Human and animal infections with *Mycobacterium microti*, Scotland. *Emerging Infectious Diseases* **13**, 1924-1927
Feldman, L. A. & Dogan, L. A. (2007) Diagnostic uses of Pax5 immunohistochemistry. *Advances in Anatomic Pathology* **14**, 323-334
Flynn, J. L., Goldstein, M. M., Chan, J., *et al*. (1995) Tumor necrosis factor-α is required in the protective immune response against *Mycobacterium tuberculosis* in mice. *Immunity* **2**, 561-572
Francis, R. J., Butler, R. E. & Stewart, G. R. (2014) *Mycobacterium tuberculosis* ESAT-6 is a leukocidin causing Ca2+ influx, necrosis and neutrophil extracellular trap formation. *Cell Death and Disease* **5**, e1474
Frota, C. C., Hunt, D. M., Buxton, R. S., *et al*. (2004) Genome structure in the vole bacillus, *Mycobacterium microti*, a member of the *Mycobacterium tuberculosis* complex with a low virulence for humans. *Microbiology* **150**, 1519-1527
Ganbat, D., Seehase, S., Richter, E., *et al*. (2016) Mycobacteria infected different cell types in the human lung and cause species dependent cellular changes in infected cells. *BMC Pulmonary Medicine* **16**, 19
García-Jiménez, W. L., Fernández-Llario, P., Gómez, L., *et al*. (2012) Histological and immunohistochemical characterisation of *Mycobacterium bovis* induced granulomas in naturally infected fallow deer (*Dama dama*). *Veterinary Immunology and Immunopathology* **149**, 66-75
García-Jiménez, W. L., Salguero, F. J., Fernández-Llario, P., *et al*. (2013) Immunopathology of granulomas produced by *Mycobacterium bovis* in naturally infected wild boar. *Veterinary Immunology and Immunopathology* **156**, 54-63
Geldmacher, C., Schuetz, A., Ngwenyama, N., *et al*. (2008) Early depletion of *Mycobacterium tuberculosis*-specific T helper 1 cell responses after HIV-1 infection. *The Journal of Infectious Diseases* **198**, 1590-1598
Gunn-Moore, D. A. (2014) Feline mycobacterial infections. *The Veterinary Journal* **201**, 230-238
Gunn-Moore, D. A., Mcfarland, S. E., Brewer, J. I., *et al*. (2011a) Mycobacterial disease in cats in Great Britain: I. culture results, geographical distribution and clinical presentation of 339 cases. *Journal of Feline Medicine and Surgery* **13**, 934-944
Gunn-Moore, D. A., Mcfarland, S. E., Schock, A., *et al*. (2011b) Mycobacterial disease in a population of 339 cats in Great Britain: II. Histopathology of 225 cases, and treatment and outcome of 184 cases. *Journal of Feline Medicine and Surgery* **13**, 945-952
Gunn-Moore, D. A., Gaunt, C. & Shaw, D. J. (2013) Incidence of mycobacterial infections in cats in Great Britain: estimate from feline tissue samples submitted to diagnostic laboratories. *Transboundary and Emerging Diseases* **60**, 338-344
Guzman, E., Price, S., Poulsom, H., *et al*. (2012) Bovine γδ T cells: cells with multiple functions and important roles in immunity. *Veterinary Immunology and Immunopathology* **148**, 161-167
Kipar, A., Schiller, I. & Baumgärtner, W. (2003) Immunopathological studies on feline cutaneous and (muco)cutaneous mycobacteriosis. *Veterinary Immunology and Immunopathology* **91**, 169-182
Kipar, A., Burthe, S. J., Hetzel, U., *et al*. (2014) *Mycobacterium microti* tuberculosis in its maintenance host, the field vole (*Microtus agrestis*): characterization of the disease and possible routes of transmission. *Veterinary Pathology* **51**, 903-914
Kramnik, I., Dietrich, W. F., Demant, P., *et al*. (2000) Genetic control of resistance to experimental infection with virulent *Mycobacterium tuberculosis*. *Proceedings of the National Academy of Sciences of the United States of America* **97**, 8560-8565
Krishnan, N., Robertson, B. D. & Thwaites, G. (2010) The mechanisms and consequences of the extra-pulmonary dissemination of *Mycobacterium tuberculosis*. *Tuberculosis* **90**, 361-366
Lalor, S. M., Clark, S., Pink, J., *et al*. (2017) Tuberculosis joint infections in four domestic cats. *JFMS Open Reports* **3**, 1-8
Landolt, P., Stephan, R., Stevens, M. J. A., *et al*. (2019) Three-reaction high-resolution melting assay for rapid differentiation of *Mycobacterium tuberculosis* complex members. *Microbiology Open* **8**, e919
Laster, S. M., Wood, J. G. & Gooding, L. R. (1988) Tumor necrosis factor can induce both apoptic and necrotic forms of cell lysis. *The Journal of Immunology* **141**, 2629-2634
Latimer, K. S., Crowell, W. A., Duncan, J. R., *et al*. (1997) Disseminated *Mycobacterium avium* complex infection in a cat: presumptive diagnosis by blood smear examination. *Veterinary Clinical Pathology* **26**, 85-89
Malik, R., Hughes, M. S., James, G., *et al*. (2002) Feline leprosy: two different clinical syndromes. *Journal of Feline Medicine and Surgery* **4**, 43-59
Martin, C. J., Carey, A. F. & Fortune, S. M. (2016) A bug's life in the granuloma. *Seminars in Immunopathology* **38**, 213-220
Martinez, F. O. & Gordon, S. (2014) The M1 and M2 paradigm of macrophage activation: time for reassessment. *F1000 Prime Reports* **6**, 13
McBride, R., Sloma, E. A., Erb, H. N., *et al*. (2017) Immune cell infiltration in feline meningioma. *Journal of Comparative Pathology* **156**, 162-168
Meeks, C., Levy, J. K., Crawford, P. C., *et al*. (2008) Chronic disseminated *Mycobacterium xenopi* infection in a cat with idiopathic CD4+ T lymphocytopenia. *Journal of Veterinary Internal Medicine* **22**, 1043-1047
Mellor, P. J., Haugland, S., Smith, K. C., *et al*. (2008) Histopathologic, immunohistochemical, and cytologic analysis of feline myeloma-related disorders: further evidence of primary extramedullary development in the cat. *Veterinary Pathology* **45**, 159-173
Michelet, L., De Cruz, K., Zanella, G., *et al*. (2015) Infection with *Mycobacterium microti* in animals in France. *Journal of Clinical Microbiology* **53**, 981-985
Miller, M. A. & Zachary, J. F. (2017) Mechanisms and morphology of cellular injury, adaptation, and death. In: Pathologic Basis of Veterinary Disease. 6th edn. Ed J. F. ZACHARY. Elsevier, St Louis, MO
Monies, R. J., Cranwell, M. P., Palmer, N., *et al*. (2000) Bovine tuberculosis in domestic cats. *Veterinary Record* **146**, 407-408
O'Brien, C. R., Malik, R., Globan, M., *et al*. (2017) Feline leprosy due to *Mycobacterium lepraemurium*: further clinical and molecular characterisation of 23 previously reported cases and an additional 42 cases. *Journal of Feline Medicine and Surgery* **19**, 737-746
O'CONNOR, C. M., Abid, M., Walsh, A. L., *et al*. (2019) Cat-to-human transmission of *Mycobacterium bovis*, United Kingdom. *Emerging Infectious Diseases* **25**, 2284-2286
O'Garra, A., Redford, P. S., Mcnab, F. W., *et al*. (2013) The immune response in tuberculosis. *Annual Review of Immunology* **31**, 475-527
O'Halloran, C. & Gunn-Moore, D. (2017) Mycobacteria in cats: an update. *In Practice* **39**, 399-406
O'Halloran, C., Mcculloch, L., Rentoul, L., *et al*. (2018) Cytokine and chemokine concentrations as biomarkers of feline mycobacteriosis. *Scientific Reports* **8**, 17314
O'Halloran, C., Ioannidi, O., Reed, N., *et al*. (2019) Tuberculosis due to *Mycobacterium bovis* in pet cats associated with feeding a commercial raw food diet. *Journal of Feline Medicine and Surgery* **21**, 667-681
Pagán, A. J. & Ramakrishnan, L. (2018) The formation and function of granulomas. *Annual Review of Immunology* **36**, 639-665
Palmer, M. V., Waters, W. R. & Thacker, T. C. (2007) Lesion development and immunohistochemical changes in granulomas from cattle experimentally infected with *Mycobacterium bovis*. *Veterinary Pathology* **44**, 863-874
Pereira-Suárez, A. L., Estrada-Chávez, C., Arriaga-Díaz, C., *et al*. (2006) Coexpression of NRAMP1, iNOS, and nitrotyrosine in bovine tuberculosis. *Veterinary Pathology* **43**, 709-717
Pérez De Val, B., Sanz, A., Soler, M., *et al*. (2019) *Mycobacterium microti* infection in free-ranging wild boar, Spain, 2017-2019. *Emerging Infectious Diseases* **25**, 2152-2154
Pierezan, F., Mansell, J., Ambrus, A., *et al*. (2014) Immunohistochemical expression of ionized calcium binding adapter molecule 1 in cutaneous Histiocytic proliferative neoplastic and inflammatory disorders of dogs and cats. *Journal of Comparative Pathology* **151**, 347-351
Reppas, G., Fyfe, J., Foster, S., *et al*. (2013) Detection and identification of mycobacteria in fixed stained smears and formalin-fixed paraffin-embedded tissues using PCR. *Journal of Small Animal Practice* **54**, 638-646
Rhodes, S. G., Gruffydd-Jones, T., Gunn-Moore, D., *et al*. (2008) Adaptation of IFN-gamma ELISA and ELISPOT tests for feline tuberculosis. *Veterinary Immunology and Immunopathology* **124**, 379-384
Rhodes, S. G., Gunn-Moore, D., Boschiroli, M. L., *et al*. (2011) Comparative study of IFNγ and antibody tests for feline tuberculosis. *Veterinary Immunology and Immunopathology* **144**, 129-134
Richter, E., Weizenegger, M., Rüsch-Gerdes, S., *et al*. (2003) Evaluation of genotype MTBC assay for differentiation of clinical *Mycobacterium tuberculosis* complex isolates. *Journal of Clinical Microbiology* **41**, 2672-2675
Ridley, D. (1964) Bacterial indices. In: Leprosy in Theory and Practice. 2nd edn. Eds R. Cochrane and T. Davey. Bristol, UK, John Wright and Sons
Roach, D. R., Bean, A. G. D., Demangel, C., *et al*. (2002) TNF regulates chemokine induction essential for cell recruitment, granuloma formation, and clearance of mycobacterial infection. *The Journal of Immunology* **168**, 4620-4627
Rodriguez-Campos, S., Smith, N. H., Boniotti, M. B., *et al*. (2014) Overview and phylogeny of *Mycobacterium tuberculosis* complex organisms: implications for diagnostics and legislation of bovine tuberculosis. *Research in Veterinary Science* **97**, S5-S19
RStudio Team 2018. RStudio: Integrated Development for R. 1.2.1335 ed. Boston, MA, USA: RStudio, Inc.

Rugtveit, J., Scott, H., Halstensen, T. S., *et al*. (1996) Expression of the L1 antigen (calprotectin) by tissue macrophages reflects recent recruitment from peripheral blood rather than upregulation of local synthesis: implications for regection diagnosis in formalin-fixed kidney specimens. *Journal of Pathology* **180**, 194-199
Salguero, F. J., Gibson, S., Garcia-Jimenez, W., *et al*. (2017) Differential cell composition and cytokine expression within lymph node granulomas from BCG-vaccinated and non-vaccinated cattle experimentally infected with *Mycobacterium bovis*. *Transboundary and Emerging Diseases* **64**, 1734-1749
Sanchez, J., Tomás, L., Ortega, N., *et al*. (2011) Microscopical and immunological features of tuberculoid granulomata and cavitary pulmonary tuberculosis in naturally infected goats. *Journal of Comparative Pathology* **145**, 107-117
Santa Cruz, D. J. & Strayer, D. S. (1982) The histologic spectrum of the cutaneous mycobacterioses. *Human Pathology* **13**, 485-495
Schindelin, J., Arganda-Carreras, I., Frise, E., *et al*. (2012) Fiji: an open-source platform for biological-image analysis. *Nature Methods* **98**, 676-682
Schluger, N. & Rom, W. (1998) The host immune response to tuberculosis. *American Journal of Respiratory and Critical Care Medicine* **157**, 679-691
Schneider, C. A., Rasband, W. S. & Eliceiri, K. W. (2012) NIH Image to ImageJ: 25 years of image analysis. *Nature Methods* **9**, 671-675
Seiler, P., Ulrichs, T., Bandermann, S., *et al*. (2003) Cell-wall alterations as an attribute of *Mycobacterium tuberculosis* in latent infection. *The Journal of Infectious Diseases* **188**, 1326-1331
Shah, K. K., Pritt, B. S. & Alexander, M. P. (2017) Histopathologic review of granulomatous inflammation. *Journal of Clinical Tuberculosis and Other Mycobacterial Diseases* **7**, 1-12
Smith, N. H., Crawshaw, T., Parry, J., *et al*. (2009) *Mycobacterium microti*: more diverse than previously thought. *Journal of Clinical Microbiology* **47**, 2551-2559
Stavinohova, R., O'Halloran, C., Newton, J. R., *et al*. (2019) Feline ocular mycobacteriosis: clinical presentation, histopathological features, and outcome. *Veterinary Pathology* **56**, 749-760
Turner, O. C., Basaraba, R. J. & Orme, I. M. (2003) Immunopathogenesis of pulmonary granulomas in the Guinea pig after infection with *Mycobacterium tuberculosis*. *Infection and Immunity* **71**, 864-871
Vallejo, R., García Marín, J. F., Juste, R. A., *et al*. (2018) Immunohistochemical characterization of tuberculous lesions in sheep naturally infected with *Mycobacterium bovis*. *BMC Veterinary Research* **14**, 154
Van Crevel, R., Ottenhoff, T. H. M. & Van Der Meer, J. W. M. (2002) Innate immunity to *Mycobacterium tuberculosis*. *Clinical Microbiology Reviews* **15**, 294-309
Van Der Kroef, M., Carvalheiro, T., Rossato, M., *et al*. (2020) CXCL4 triggers monocytes and macrophages to produce PDGF-BB, culminating in fibroblast activation: implications for systemic sclerosis. *Journal of Autoimmunity* **111**, 102444-102444
Van Soolingen, D., Van Der Zanden, A. G. M., De Haas, P. E. W., *et al*. (1998) Diagnosis of *Mycobacterium microti* infections among humans by using novel genetic markers. *Journal of Clinical Microbiology* **36**, 1840-1845
Volkman, H. E., Clay, H., Beery, D., *et al*. (2004) Tuberculous granuloma formation is enhanced by a *Mycobacterium* virulence determinant. *PLoS Biology* **2**, e367
Wangoo, A., Johnson, L., Gough, J., *et al*. (2005) Advanced granulomatous lesions in *Mycobacterium bovis*-infected cattle are associated with increased expression of type I Procollagen, γδ (WC1+) T cells and CD 68+ cells. *Journal of Comparative Pathology* **133**, 223-234
Zwadlo, G., Bröcker, E.-B., Von Bassewitz, D.-B., *et al*. (1985) A monoclonal antibody to a differentiation antigen present on mature human macrophages and absent from monocytes. *Journal of Immunology* **134**, 1487-1492
Zwadlo, G., Schlegel, R. & Sorg, C. (1986) A monoclonal antibody to a subset of human monocytes found only in the peripheral blood and inflammatory tissues. *Journal of Immunology* **137**, 512-518

Supporting Information

The following supporting information is available for this article:

Appendix S1. Macro scripts used for quantifying positive staining for collagen (Masson's Trichrome) and immunohistochemical markers.